Journal of Hazardous Materials 213–214 (2012) 100–108

Contents lists available at SciVerse ScienceDirect

Journal of Hazardous Materials

journal homepage: www.elsevier.com/locate/jhazmat

Competitive adsorption characteristics of fluoride and phosphate on calcined Mg–Al–CO_3 layered double hydroxides

Peng Cai, Hong Zheng*, Chong Wang, Hongwen Ma, Jianchao Hu, Yubing Pu, Peng Liang

School of Materials Science and Technology, China University of Geosciences, Beijing 100083, PR China

ARTICLE INFO

Article history:
Received 23 September 2011
Received in revised form 4 January 2012
Accepted 20 January 2012
Available online 27 January 2012

Keywords:
Calcined Mg–Al–CO_3
Layered double hydroxides
Competitive adsorption
Fluoride
Phosphate

ABSTRACT

With synthetic wastewater, competitive adsorption characteristics of fluoride and phosphate on calcined Mg–Al–CO_3 layered double hydroxides (CLDH) were investigated. A series of batch experiments were performed to study the influence of various experimental parameters, such as pH, contact time, and order of addition of the anions on the competitive adsorption of fluoride and phosphate on CLDH. It was found that the optimal pH is around 6 and it took 24 h to attain equilibrium when fluoride and phosphate were simultaneous added. The order of addition of anions influenced the adsorption of fluoride and phosphate on CLDH. The kinetic data were analyzed using the pseudo first-order and pseudo second-order models and they were found to fit very well the pseudo second-order kinetic model. Data of equilibrium experiments were fitted well to Langmuir isotherm and the competitive monolayer adsorption capacities of fluoride and phosphate were found to be obviously lower than those of single anion at 25 °C. The results of X-ray diffraction, Scanning Electron Microscopy with energy-dispersive X-ray analyses, and ATR-FTIR demonstrate that the adsorption mechanism involves the rehydration of mixed metal oxides and concomitant intercalation of fluoride and phosphate ions into the interlayer to reconstruct the initial LDHs structure.

1. Introduction

Fluorine is an essential element for human health. Moderate fluoride (0.5–1.5 mg/L) in drinking water is an essential micronutrient for the calcification of the dental enamel and bone formation [1]. However, excessive intake of fluoride not only causes dental and skeletal fluorosis, but may also lead to mutations in the user's deoxyribonucleic acid [2]. The contamination of fluoride in ground and surface water could come either from natural geological sources including various minerals, such as fluorite, biotites, topaz, and their corresponding host rocks, such as granite, basalt, syenite, and shale [3] or from industries that use fluoride-containing compounds as raw materials, e.g., glass and ceramic production, semiconductor manufacturing, electroplating, coal fired power stations, beryllium extraction plants, brick and iron works, and aluminium smelters [4]. Phosphorus can provide an additional nutrient for growth of photosynthetic macro- and microorganisms in aquatic bodies, and also leads to an eutrophication problem especially in enclosed water bodies [5]. Various industries produce wastewater that contains high concentration of phosphorus and fluoride, such as fertilizer, semiconductor, and phosphoric acid processing [6–9]. Hence, it is necessary to use an effective and robust technique for the removal of excess fluoride and phosphate from water.

There are many methods for defluoridation of water, i.e. precipitation–coagulation [10], adsorption [11,12], Donnan dialysis [13], electrodialysis [14], reverse osmosis [9,15], nanofiltration [16], electrolytic defluoridation [17], and ultrafiltration [18]. For phosphate removal, various techniques including chemical precipitation, biological treatment, crystallization treatment [19], and methods such as electrocoagulation [20], microfiltration [21], membrane bioreactors [22], nanofiltration, reverse osmosis [23–25], and adsorption [26] have been used. Fluoride and phosphate also can be simultaneously removed by some novel methods, such as nanomagnetite aggregation process [27], hybrid precipitation–microfiltration process [28], and RO/NF treatment [29]. Among these potential separation technologies mentioned above, adsorption is arguably one of the most promising methods because of its initial cost, flexibility and simplicity of design and ease of operation and maintenance for removing fluoride and phosphate from water [26,30].

Layered double hydroxides (LDHs) are a class of naturally occurring and synthetic anionic clays, also known as hydrotalcite-like compounds in which divalent cations within brucite-like layers are replaced by trivalent cations. The resulting positive charge is compensated by hydrated anions located in the interlayer space between two brucite sheets. The general formula can be normally expressed as $[M_{1-x}^{2+}M_x^{3+}(OH)_2]^{x+}(A^{n-})_{x/n}\cdot mH_2O$, where M^{2+} and

* Corresponding author. Tel.: +86 10 82322759; fax: +86 10 82322974.
E-mail address: zhengh@cugb.edu.cn (H. Zheng).

0304-3894/$ – see front matter © 2012 Elsevier B.V. All rights reserved.
doi:10.1016/j.jhazmat.2012.01.069

M^{3+} are di- and trivalent metal cations that occupy octahedral sites in the hydroxide layers, A^{n-} is an exchangeable anion, and x is equal to the molar ratio of $M^{3+}/(M^{2+}+M^{3+})$ and the layer charge will depend on the M^{2+}/M^{3+} ratio [31]. The value of x is reported to be 0.2–0.4 in forming a pure LDHs phase. If x values are outside this range, hydroxides or other compounds as impurities may be formed [32]. The LDHs materials have received increasing attention because of their many applications as precursors to magnetic materials [33], catalysts [34], and anion exchangers [35–37]. Due to the large surface areas (20–120 m^2/g) and high anion-exchange capacities (3.0–4.8 meq/g), LDHs have been studied as potential adsorbents for removing toxic anionic species from aqueous systems [38–40]. The selective binding of anions by LDHs is affected to a considerable extent by the properties of the anions. Generally, LDHs have affinities for anions following the order of the Hofmeister series [41]. That is, the affinity increases with increasing charge and decreasing ionic radius. For example, the affinity for monovalent inorganic anions decreases in the order of $OH^- > F^- > Cl^- > Br^- > NO_3^- > I^-$. LDHs generally have greater affinity for multivalent inorganic anions compared with monovalent inorganic anions. The CO_3^{2-} is the most preferentially adsorbed, which significantly inhibits further ion exchange [42]. Moreover, the interlayer CO_3^{2-} anion can be removed by being calcined at a certain temperature (below 800 °C). The calcined Mg–Al–CO_3 LDHs (CLDH) was found to be better adsorbents with higher adsorption capacity for removal of hazardous anions from contaminated water since the calcination of LDHs containing carbonate as interlayer anion causes the formation of $M^{II}M^{III}O$ solid solution capable of recovering the LDHs layered structure upon treatment with water or aqueous solution containing various anions [43–45]. It is called the memory effect that the oxide obtained at the intermediate calcination temperature (<600 °C) can easily regain the layered structure to become a similar LDHs compound upon exposure to aqueous solution [46,47].

In this work, we attempt to use calcined Mg–Al–CO_3 LDHs as an adsorbent to simultaneously remove fluoride and phosphate from aqueous solution. The objective of this work was to investigate the influencing factors, isotherm and kinetic modeling of competitive adsorption of fluoride and phosphate on calcined Mg–Al–CO_3 LDHs and reveal the competitive adsorption characteristics of fluoride and phosphate on calcined Mg–Al–CO_3 LDHs. The competitive adsorption characteristics are important to predict the adsorption process of various anions.

2. Materials and methods

2.1. Synthesis of calcined Mg–Al–CO_3 LDHs

The layered double hydroxides containing carbonate as the interlayer anion was synthesized by a modified co-precipitation method as described elsewhere [40]. The method involves very rapid mixing to complete the nucleation process, followed by a separate aging process. Analytical grade $Mg(NO_3)_2{\cdot}6H_2O$ (0.09 mol) and $Al(NO_3)_3{\cdot}9H_2O$ (0.045 mol) were dissolved in deionized water. A second solution containing analytical grade NaOH (0.31 mol) and Na_2CO_3 (0.13 mol) in deionized water was prepared. The two solutions were simultaneously added to a DJ-2S high speed mixer with rotor speed of 6000 rpm and stirred for 5 min. The resulting slurry was removed from high speed mixer and aged at 100 °C for a specified period. The final precipitate was filtered, washed thoroughly, and dried at 80 °C for 24 h to obtain Mg–Al–CO_3 LDHs. Calcined Mg–Al–CO_3 LDHs (CLDH) was obtained by calcining LDHs in a muffle furnace at 500 °C for 3 h. The magnesium and aluminium contents of the samples were determined by an inductively coupled plasma optical emission spectroscopy (ICP-OES) instrument (Perkin Elmer Optima 2000DV) after appropriate dissolution of the solid samples. The carbon and hydrogen contents of the Mg–Al–CO_3 LDHs were obtained in an elemental analyzer (Vario EL). Based on the results of the chemical analysis, the empirical formulae of synthesized Mg–Al–CO_3 LDHs and CLDH were found to be $[Mg_{0.68}Al_{0.32}(OH)_2](CO_3)_{0.16}{\cdot}0.412H_2O$ and $Mg_{0.67}Al_{0.33}O_{1.165}$, respectively. The x value (0.32) was found in the range of 0.2–0.4, indicating that a pure LDHs phase is formed [32]. The specific surface areas of the Mg–Al–CO_3 LDHs and CLDH are 82.5 m^2/g and 143.0 m^2/g, respectively, which were measured by the BET method with N_2 gas.

2.2. Competitive adsorption of fluoride and phosphate on CLDH

Analytical grade NaF, KH_2PO_4, and deionized water were used in the preparation of the stock NaF and KH_2PO_4 solutions. The stock solutions were diluted to prepare for working solutions. The pH value was adjusted by addition of 0.1 M NaOH and/or 0.1 M HNO_3 to designed value.

The batch adsorption experiments were carried out in a serial of 100 mL plug-contained conical flasks with variation of solution pH (3.0–11.0), adsorbate concentration (5–50 mg/L), and contact time (15 min to 48 h). Solutions of NaF and KH_2PO_4 were mixed with a CLDH suspension to give a final concentration of 0.5 g/L of CLDH. $NaNO_3$ was added as the background electrolyte (10 mM). The bottles were shaken in HZS-H air bath and constant temperature oscillator at a speed of 150 round per min and a temperature of 25 ± 0.2 °C. Water samples in conical flasks were centrifuged at 5000 round per min for 10 min and filtered with a 0.45 μm membrane for the analysis of the concentrations of residual fluoride and phosphate in solution.

Competitive adsorption of fluoride and phosphate on CLDH in the presence of another one was also conducted using different order of addition of the adsorbates. In the first case, fluoride was added to the CLDH suspension and the mixture was shaken at 25 °C for 24 h. Then, phosphate solution was added and the system was shaken for another 24 h. This system was designated as (fluoride-CLDH)-phosphate. In the second case, the same procedure was applied but phosphate was brought to contact with CLDH first and the system was designated as (phosphate-CLDH)-fluoride. In the third case, fluoride and phosphate were brought to contact with CLDH simultaneously.

The concentration of fluoride ion in the solutions was determined using a fluoride ion-selective electrode, which measures concentrations from 10^{-6} μM to saturated solutions. Phosphate concentration in the solutions was determined by the molybdate blue method. The concentration of phosphate was obtained by colorimetric reading of a spectrophotometer (722S Spectrophotometer) at a wavelength of 700 nm [48]. The amount of fluoride and phosphate adsorbed was calculated by the difference between the initial and final concentrations.

2.3. Characterization of samples before and after the adsorption of fluoride and phosphate ions

The CLDH materials before and after the adsorption of fluoride and phosphate ions were characterized by X-ray diffraction (XRD), Scanning Electron Microscopy (SEM) with energy-dispersive X-ray analyses (EDX), and ATR-FTIR. XRD patterns were obtained at the scan speed of 8°/min with CuKα radiation at 40 kV and 100 mA. SEM images and EDX analyses were taken on a Hitachi S4800 Field-Emission Scanning Electron Microscope. ATR-FTIR spectra were recorded using a Nicolet 5700 infrared spectrometer with a deuterated triglycine sulfate (DTGS) detector and a ZnSe horizontal ATR cell. Infrared spectra over the 4000–650 cm^{-1} range were obtained by averaging 32 scans with a resolution of 4 cm^{-1} at room

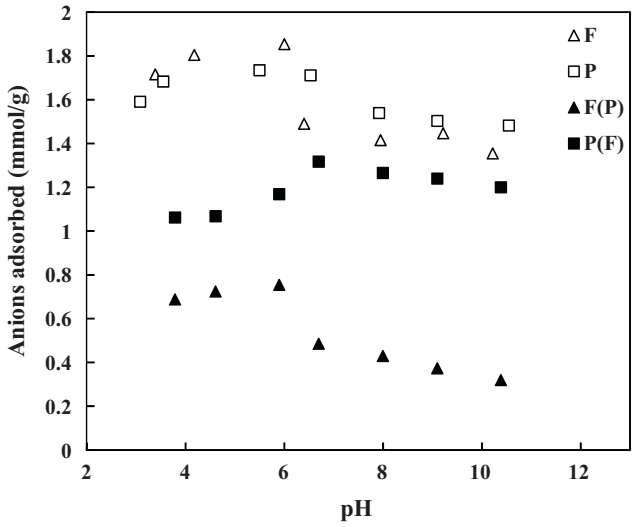

Fig. 1. Effect of pH values on fluoride and phosphate adsorption on CLDH ($C_{0(F)}$ = 2.6 mmol/L, $C_{0(P)}$ = 1.6 mmol/L, adsorbent dosage 0.5 g/L, shaking time 24 h, temperature 25 ± 0.2 °C).

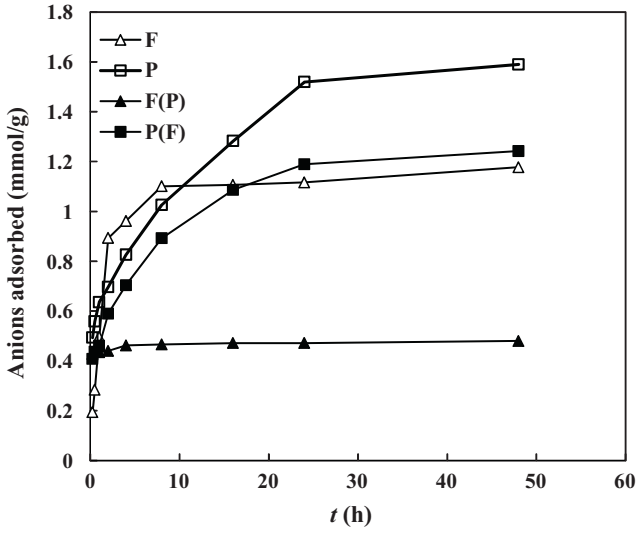

Fig. 2. Effect of contact time on fluoride and phosphate adsorption on CLDH ($C_{0(F)}$ = 1.6 mmol/L, $C_{0(P)}$ = 1.0 mmol/L, adsorbent dosage 0.5 g/L, pH = 6.0 ± 0.1, temperature 25 ± 0.2 °C).

temperature (298 K). Data collection and spectral calculations were accomplished using OPUS software. In order to remove the strong spectral contribution of water, all final ATR-FTIR spectra of wet pastes were processed by subtracting the spectrum of the corresponding filtered suspension supernatants from the spectrum of the measured sample.

3. Results and discussion

3.1. Effect of solution pH value on fluoride and phosphate adsorption

The pH-dependent single-component adsorption of fluoride and phosphate was investigated at a constant ionic strength, as shown in Fig. 1. The amount of fluoride or phosphate adsorbed on CLDH is maximum when pH is around 6.0, reaching 1.85 mmol/g for fluoride and 1.73 mmol P/g for phosphate. It is obvious that fluoride or phosphate ions are adsorbed more at lower pH than at higher pH and the change is greater for fluoride ion than phosphate ions. These results can be attributed to presence of excess OH^- ions competing with fluoride or phosphate at higher pH value. The concentration of OH^- ion is improved and phosphate exists as multivalent anions at higher pH values. According to the order of the Hofmeister series [41], LDHs have greater affinities for OH^- compared with F^- and greater affinity for multivalent phosphate anions compared with monovalent OH^- anion. On the other hand, a higher pH can cause the adsorbent surface to carry more negative charges and thus would generate repulsive interaction between the adsorbent surface and the anions in solution. In acid pH range 3–6, CLDH can be easily rehydrated and incorporate fluoride and phosphate anions to rebuild the initial layered structure by means of the so-called "memory effect" because of less competition of OH^- ion. Moreover, most carbonate was removed after calcined at 500 °C and little CLDH will be eliminated as CO_2. When the pH is too low, because the layered material may be partly dissolved, adsorption capacity can be lead to a decrease [45].

Anion adsorption in competitive systems is affected directly by competition for the activate sites and indirectly by the change in the electrostatic charge in the plane of adsorption [49]. Fluoride adsorption in the presence of phosphate and phosphate adsorption affected by the presence of fluoride as a function of pH is also shown in Fig. 1. The simultaneous addition of fluoride and phosphate resulted in a significant decrease in the adsorption of fluoride throughout the pH range investigated, but more fluoride is adsorbed at lower pH than at higher pH values, which is in accordance with single-component adsorption. A significant decrease for fluoride implied that fluoride was unable to compete effectively with phosphate even if the initial concentration of fluoride (2.6 mmol/L) was higher than that of phosphate (1.6 mmol/L) and pH values are lower. This is different from the LDHs affinity order of $F^- > H_2PO_4^-$ reported by Ulibarri and Hermosín [50]. The possible reason is that fluoride and phosphate anions can not only be incorporated to rebuild the initial layered structure by CLDH, but also be adsorbed by CLDH surface. Moreover, the slightly pH increasing during the adsorption can cause the formation of multivalent HPO_4^{2-}. On the other hand, the adsorption of phosphate obviously decreased at lower pH values and a little decreased at higher pH values. Just as mentioned previously, phosphate exists as multivalent anions at higher pH values. LDHs have greater affinities for multivalent phosphate anions compared with monovalent F^- anion. However, phosphate exists as monovalent $H_2PO_4^-$ at lower pH values. Monovalent anion is adsorbed more difficult than multivalent anions [45]. When the activate site is limited, the adsorption of $H_2PO_4^-$ is suppressed by the competition of F^-. At the pH around 6.0, the adsorption capacity of fluoride decreased from 1.85 mmol/g to 0.75 mmol/g, while the adsorption capacity of phosphate only decreased from 1.73 mmol P/g to 1.17 mmol P/g. As fluoride was unable to compete effectively with phosphate, the phosphate interacted more strongly with CLDH than fluoride did, meaning that once phosphate was adsorbed first on CLDH, it is more difficult to be displaced by fluoride.

3.2. Effect of contact time on fluoride and phosphate adsorption

In order to determine the equilibration time for adsorption of fluoride and phosphate and to investigate the kinetics of adsorption process, the adsorption of fluoride and phosphate on CLDH in single or binary system as a function of contact time was studied. A plot between time and amount of fluoride and phosphate adsorbed is shown in Fig. 2. From Fig. 2, we can see that the adsorption of fluoride and phosphate on CLDH is rapid in the beginning, followed by a slower process to reach a plateau. Near equilibrium is achieved in less than 24 h, hence the equilibrium time of 24 h was applied for the study of adsorption isotherms. Fig. 2 demonstrates that the

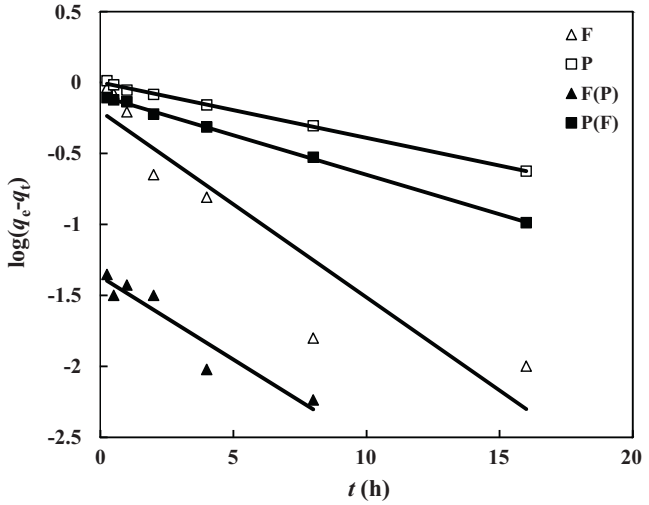

Fig. 3. Pseudo first-order adsorption kinetics of fluoride and phosphate on CLDH.

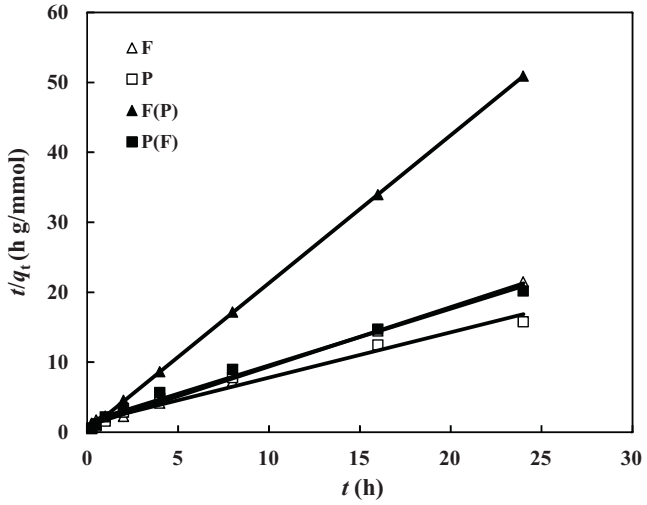

Fig. 4. Pseudo second-order adsorption kinetics of fluoride and phosphate on CLDH.

adsorption capacity of fluoride or phosphate in the single system is larger than that in the binary system, which indicates the presence of phosphate or fluoride reduced the adsorption of another one on CLDH. It is also very interesting that it took less time for fluoride to reach equilibrium when it is in binary system, the presence of phosphate may be the driving force leading to a higher uptake rate for fluoride.

3.3. Adsorption kinetics

Lagergren's pseudo first-order and pseudo second-order models were used for analysis of sorption kinetics.

The Lagergren's equation for pseudo first-order kinetics can be written as follows [51]:

$$\log\ (q_e - q_t) = \log\ q_e - \frac{k_1 t}{2.303} \quad (1)$$

where q_e is the amount of adsorbate adsorbed (mmol/g) at equilibrium and q_t is the amount of adsorbate adsorbed (mmol/g) at time t, k_1 is the rate constant (h^{-1}). Pseudo first-order kinetic plotted at 25 °C is given in Fig. 3. The Lagergren's first-order rate constant (k_1) and q_e were calculated from the intercept and slope of the plot and are listed in Table 1 along with the corresponding correlation coefficients. It was observed that the pseudo first-order model did not fit well. The calculated q_e values do not agree with the experimental q_e values, suggesting that the adsorption of fluoride and phosphate on CLDH does not follow pseudo first-order kinetics.

Pseudo second-order model is represented as [52]:

$$\frac{t}{q_t} = \frac{1}{k_2 q_e^2} + \frac{1}{q_e} t \quad (2)$$

where q_e and q_t have the same meaning as mentioned previously and k_2 is the rate constant for the pseudo second-order kinetics. The plots of t/q_t versus t are shown in Fig. 4. The k_2 and q_e calculated from the model are also listed in Table 1 along with the corresponding correlation coefficients. The predicted equilibrium uptakes are close to the experimental values indicating the applicability of the pseudo second-order model.

3.4. Adsorption isotherms

The adsorption isotherms of fluoride and phosphate in single or binary system, corresponding to the simultaneous addition experiments at an ionic strength of 0.01 M, are shown in Fig. 5. The adsorption of fluoride or phosphate decreases in the presence of another one, which indicates that a competitive adsorption process between fluoride and phosphate takes place. Fluoride ion is known for its specific adsorption on CLDH, and thus the phosphate competes with fluoride for adsorption sites on CLDH.

The isotherm results of single and binary systems at a constant temperature of 25 °C were analyzed using two important isotherms: Langmuir and Freundlich isotherm models. The expression of the Langmuir model is given by Eq. (3) [53]:

$$q_e = \frac{Q_0 b C_e}{1 + b C_e} \quad (3)$$

where Q_0 and b are the Langmuir constants related to the maximum amount and energy of adsorption. q_e is the adsorption capacity at equilibrium(mmol/g) and C_e is the equilibrium concentration (mmol/L), respectively. The Langmuir equation can be described by the linearized form:

$$\frac{C_e}{q_e} = \frac{1}{Q_0} C_e + \frac{1}{Q_0 b} \quad (4)$$

The linear plot of specific sorption (C_e/q_e) against the equilibrium concentration (C_e) is shown in Fig. 6. The Langmuir constants Q_0 and b were determined from the slope and intercept of the plot and are presented in Table 2.

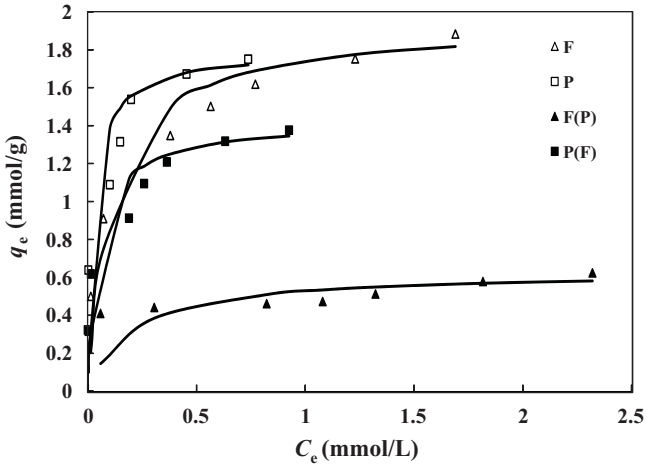

Fig. 5. Adsorption isotherms of fluoride and phosphate on CLDH (adsorbent dosage 0.5 g/L, pH = 6.0 ± 0.1, temperature 25 ± 0.2 °C).

Table 1
Comparison of pseudo first-order and pseudo second-order adsorption rate constants and calculated and experimental q_e values for single and binary systems.

System	$q_{e,exp}$ (mmol/g)	Pseudo first-order kinetic model			Pseudo second-order kinetic model		
		k_1 (1/h)	$q_{e,cal}$ (mmol/g)	R^2	k_2 (g/mmol h)	$q_{e,cal}$ (mmol/g)	R^2
F	1.12	0.30	0.63	0.866	0.78	1.18	0.998
p	1.52	0.09	1.00	0.998	0.31	1.54	0.973
F (P)	0.47	0.27	0.04	0.901	25.54	0.47	1
P (F)	1.19	0.13	0.81	0.999	0.43	1.24	0.988

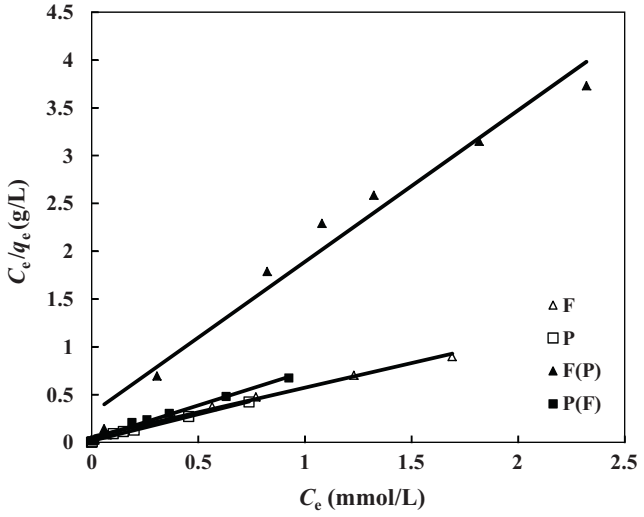

Fig. 6. Linear plots of Langmuir isotherm of fluoride and phosphate adsorption on CLDH at 25 ± 0.2 °C.

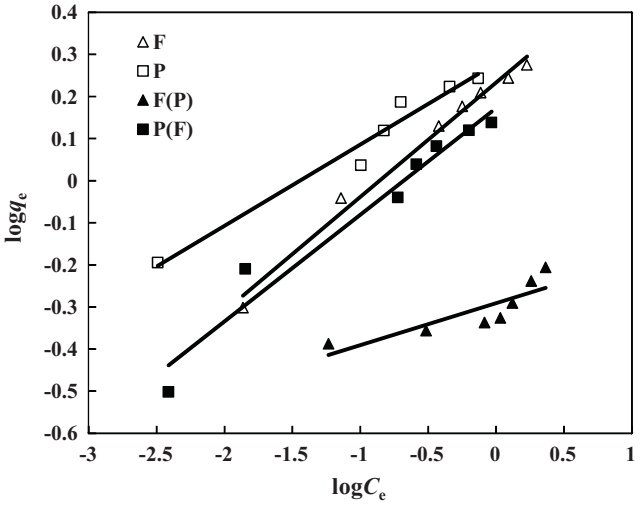

Fig. 7. Linear plots of Freundlich isotherm of fluoride and phosphate adsorption on CLDH at 25 ± 0.2 °C.

The Freundlich isotherm [54] can be applied for non-ideal sorption on heterogeneous surfaces and multilayer adsorption. The Freundlich equation is expressed as

$$q_e = K_f C_e^{1/n} \quad (5)$$

where K_f and n are the Freundlich temperature-dependent constants with K_f being the adsorption capacity and n giving an indication the favorability of the adsorption process. Values of $n > 1$ represent favorable adsorption condition. In order to determine the constants K_f and n, the Freundlich equation can be described by the linearized form:

$$\log\ q_e = \log K_f + \frac{1}{n}\log C_e \quad (6)$$

Fig. 7 shows the linear plot of Freundlich isotherm of fluoride and phosphate adsorption on CLDH at 25 °C. Values of K_f and n were calculated from the intercept and slope of the plot and are presented in Table 2.

As seen in Table 2, the Langmuir isotherm is a better model than the Freundlich isotherm on the basis of the correlation coefficients. The maximum sorption capacity of fluoride (1.94 mmol/g) in single system is much higher than that (0.63 mmol/g) in binary system and the maximum sorption capacity of phosphate (1.79 mmol/g) in single system is a little higher than that (1.42 mmol/g) in binary system, also indicating that fluoride was unable to compete effectively

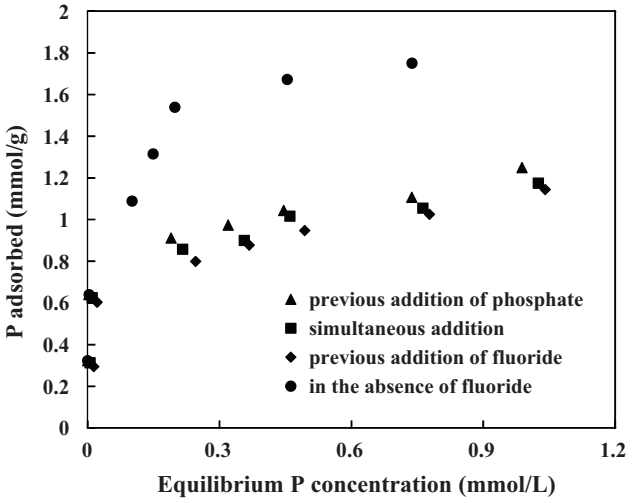

Fig. 8. Effect of the order of addition on the adsorption of phosphate by CLDH at pH 6.0 ± 0.1.

Table 2
Langmuir and Freundlich isotherm model constants and correlation coefficients for adsorption of fluoride and phosphate on CLDH.

System	Langmuir isotherm			Freundlich isotherm		
	Q_0 (mmol/g)	b (L/mmol)	R^2	K_f (mmol/g (L/mmol)$^{1/n}$)	n	R^2
F	1.94	8.74	0.992	1.71	3.68	0.988
p	1.79	33.48	0.992	1.90	5.18	0.965
F (P)	0.63	5.13	0.972	0.51	10.05	0.724
P (F)	1.42	19.53	0.990	1.50	3.95	0.958

with phosphate. The values of Freundlich constant *n* larger than 1 point out a favorable adsorption process.

3.5. Effect of order of addition on the adsorption of fluoride and phosphate by CLDH

In order to gain further insight into the mechanism of the effect of fluoride or phosphate on the adsorption of another one, different contact order of fluoride and phosphate with CLDH was applied. Fig. 8 represents phosphate adsorption at a given fluoride concentration (1.6 mmol/L) with different order of addition. The order of addition of fluoride has a little effect on the amounts of phosphate adsorbed on CLDH. When fluoride was added first, more suppression was observed than the system where phosphate was added first. The amount of phosphate adsorbed was in the following order: (phosphate-CLDH)-fluoride > phosphate-fluoride-CLDH > (fluoride-CLDH)-phosphate. Similar to phosphate adsorption, the adsorption of fluoride in the presence of phosphate (1.0 mmol/L) was also suppressed, but the suppression is more obvious. Fig. 9 shows that more fluoride was adsorbed when it was added before phosphate. Fluoride and phosphate are anions competing for similar activate sites on CLDH. Whatever was brought to contact with CLDH, they would occupy the activate site first. When the activate site is limited, there may exit an ion exchange of fluoride and phosphate according to a different contact order. However, once one of them is adsorbed, it will be hard to be displaced. For this competitive system, it is more difficult to be displaced when phosphate was adsorbed first on CLDH, also indicating fluoride was unable to compete effectively with phosphate. The possible reasons are attributed to surface adsorption on CLDH and slightly pH increasing during the adsorption.

Depending on the order of adsorbates addition, fluoride or phosphate adsorption has to reach equilibrium in different directions. For example, when only phosphate is added at the beginning of the experiment, there will be an important phosphate adsorption that should coincide with the phosphate adsorption isotherm in absence of fluoride. Afterwards, once fluoride is added, the competition between fluoride and phosphate should induce a decrease in phosphate adsorption, and equilibrium has to be reached moving from high amounts of adsorbed phosphate to lower amounts of adsorbed phosphate. This decrease in phosphate adsorption was observed when fluoride concentration is 1.6 mmol/L, indicating that some phosphate is desorbed by the presence of fluoride. On the contrary, when only fluoride is added at the beginning of the experiment, the subsequent addition of phosphate should induce a phosphate adsorption. Thus, phosphate has to be adsorbed by displacing some of the previously adsorbed fluoride, and equilibrium has to be reached moving from zero adsorbed phosphate to higher amounts of adsorbed phosphate. In the third case, simultaneous addition of both adsorbates, phosphate and fluoride should adsorb simultaneously on CLDH and compete for common sites. The phosphate adsorption isotherms of previous addition of phosphate or fluoride are different from those of simultaneous addition of the adsorbates, which indicates the real equilibrium situations are not reached. The results of the experiments also implied that when one

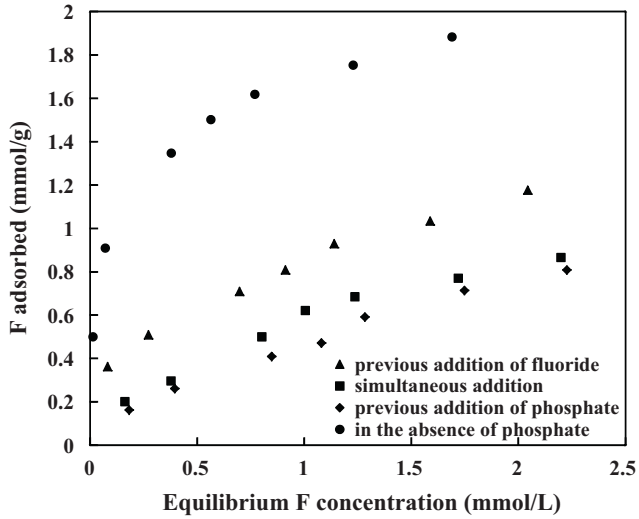

Fig. 9. Effect of the order of addition on the adsorption of fluoride by CLDH at pH 6.0 ± 0.1.

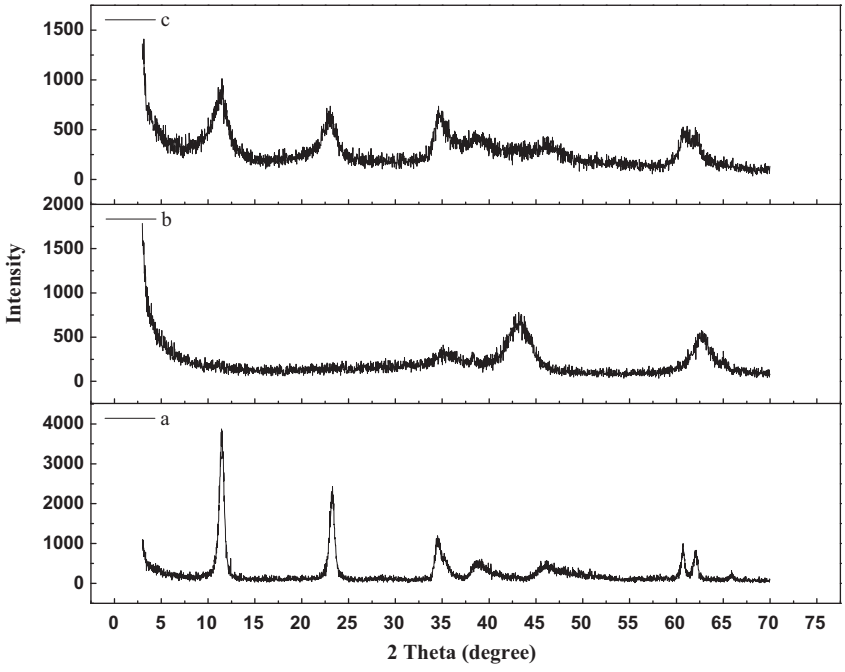

Fig. 10. XRD patterns of (a) Mg–Al–CO_3 LDHs, (b) Mg–Al–CO_3 LDHs calcined at 500 °C, and (c) CLDH after adsorption of fluoride and phosphate.

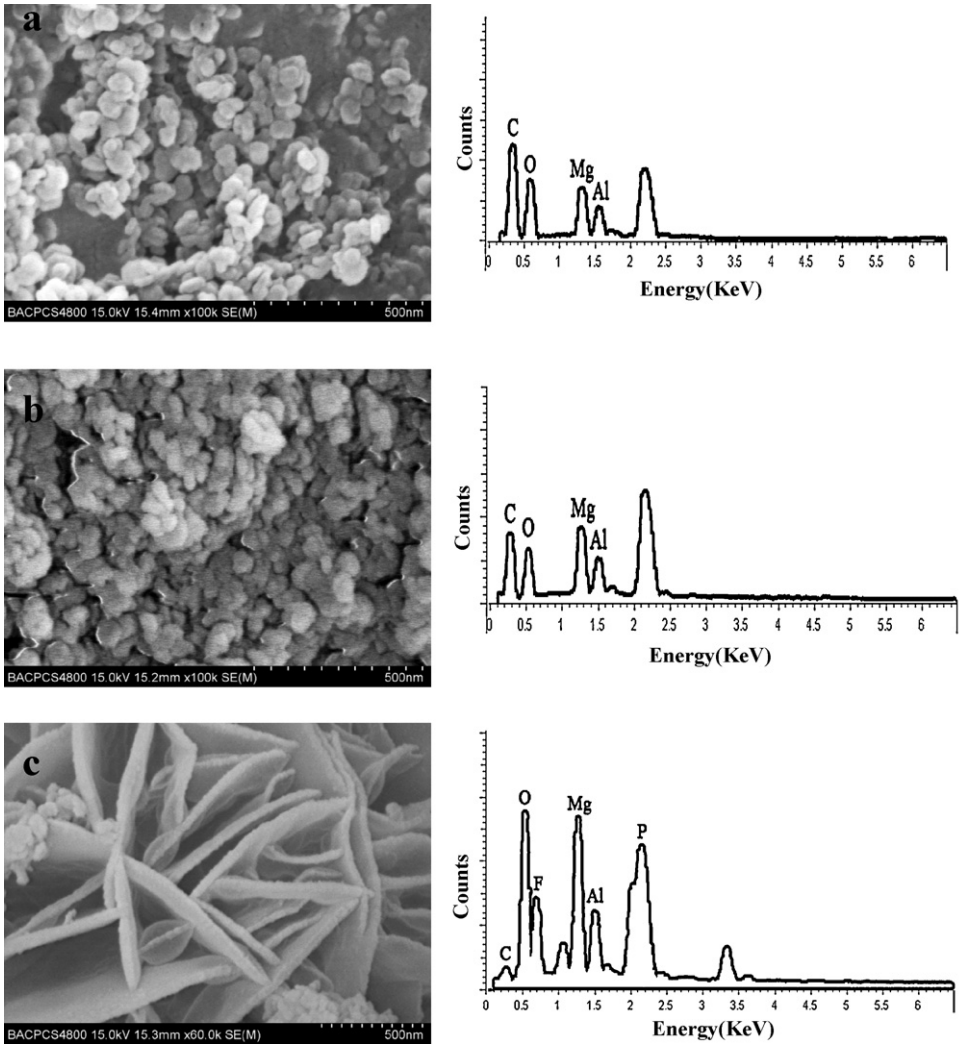

Fig. 11. SEM images and corresponding EDX spectrum of (a) Mg–Al–CO_3 LDHs, (b) Mg–Al–CO_3 LDHs calcined at 500 °C, and (c) CLDH after adsorption of fluoride and phosphate.

of the anions was added first, the desorption of this anion is rather slow and thus equilibrium is attained more slowly than in the case of simultaneous addition.

3.6. XRD, SEM, EDX, and ATR-FTIR proofs of fluoride and phosphate ions adsorption on CLDH

Fig. 10 represents XRD patterns of Mg–Al–CO_3 LDHs, CLDH, and CLDH after adsorption of fluoride and phosphate ions. The XRD patterns of Mg–Al–CO_3 LDHs exhibit the characteristic reflections of the hydrotalcite structure and accordingly, the patterns can be indexed in a hexagonal lattice with an R3m rhombohedral space group symmetry [34], further indicating the successful formation of the LDHs structure. The XRD patterns of CLDH showed the disappearance of the peaks of hydrotalcite, due to the collapse of the structure of Mg–Al–CO_3 LDHs, and the appearance of broad peaks attributed to the formation of Mg–Al mixed oxides, indicating Mg–Al–CO_3 LDHs decomposes into magnesium and aluminum oxides when heated at 500 °C. The XRD patterns of the F-P-loaded CLDH regained the characteristic reflections of the hydrotalcite structure and verified the re-construction of the layered double hydroxides structure of the material during adsorption of fluoride and phosphate from the aqueous solutions.

The particle morphology and chemical composition of the Mg–Al–CO_3 LDHs, CLDH, and CLDH after adsorption of fluoride and phosphate can be seen in the SEM images and corresponding EDX spectrum presented in Fig. 11. The SEM image of Mg–Al–CO_3 LDHs showed a layered structure and particles aggregation with lateral size 50–100 nm and corresponding EDX spectrum showed the presence of Mg, Al, C, O, also indicating Mg–Al–CO_3 LDHs was successfully prepared. The SEM micrograph of the CLDH revealed the collapsed layer structure, which further indicated the Mg–Al–CO_3 LDHs transforms to mixed magnesium and aluminum oxides. Moreover, corresponding EDX spectrum of CLDH still showed the presence of Mg, Al, C, O, although their contents are lower than those in Mg–Al–CO_3 LDHs, indicating that carbonate was not completely removed after calcined at 500 °C. This result strengthens the findings of Hibino et al. who demonstrated that 20–30% of the carbonates still remained in CLDH when Mg–Al–CO_3 LDHs was heated at 500 °C [55]. From the SEM image of CLDH after adsorption of fluoride and phosphate, the original layered structure was found partly regenerated. The appearance of the layers also verified the rebuilding of the original layered structure by incorporating anions into the collapsed layer structure and this is in accordance with the XRD results. EDX spectrum showed the presence of F and P in CLDH after adsorption of fluoride and phosphate, verifying the adsorption

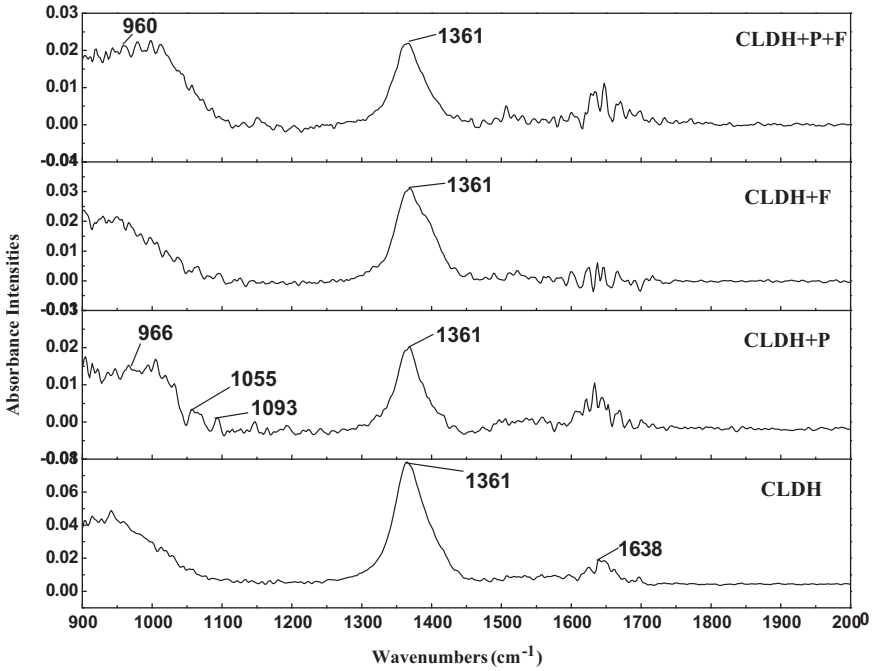

Fig. 12. ATR-FTIR spectra of CLDH, CLDH after adsorption of phosphate, CLDH after adsorption of fluoride, and CLDH after adsorption of fluoride and phosphate.

of fluoride and phosphate by CLDH. The increase in O content is due to the adsorption of phosphate.

The ATR-FTIR spectra of CLDH before and after adsorption of fluoride and phosphate ions are shown in Fig. 12. All the spectra showed a peak at about 1361 cm^{-1} attributed to carbonate species. ATR-FTIR analyses further gave an evidence that carbonate was not completely removed after heated at 500 °C. This observation is in good agreement with the EDX spectrum data. After adsorption of phosphate, peak at the wave number of 966 cm^{-1} shows symmetric stretching vibration of PO_4^{3-} and peaks at the wave number of 1055 and 1093 cm^{-1} show antisymmetric stretching vibration of PO_4^{3-}, indicating phosphate was adsorbed on CLDH. The absorbance intensities of new peaks at 1055 and 1093 cm^{-1} were very weak when phosphate and fluoride were simultaneously adsorbed on CLDH, which indicated the presence of fluoride decreased the adsorption of phosphate and competitive adsorption between fluoride and phosphate on CLDH happened.

4. Conclusions

Competitive adsorption of fluoride and phosphate on CLDH has been studied. Competition in adsorption between fluoride and phosphate was affected by pH, contact time and sequence of addition of the anions. It was found that the optimal pH is around 6 and it took 24 h to attain equilibrium when fluoride and phosphate were simultaneous added. The sequence of addition of anions influenced the adsorption of fluoride and phosphate on CLDH, more fluoride or phosphate was adsorbed when it was added before another one. Fluoride was unable to compete effectively with phosphate. Adsorption of fluoride and phosphate on CLDH follows the pseudo second-order model. The adsorption isotherm results could be fitted by the Langmuir and Freundlich isotherm models, and the former is a better model. The Freundlich constant $n > 1$ represents a favorable adsorption condition. Competition for adsorption sites was considered to be the mechanism of the adsorption of fluoride and phosphate on CLDH, since the presence of phosphate or fluoride decreases the adsorption of another one. The results of XRD, SEM, EDX, and ATR-FTIR demonstrate that the main adsorption mechanism involves the rehydration of mixed metal oxides and concomitant intercalation of fluoride and phosphate ions into the interlayer to reconstruct the initial LDHs structure.

Acknowledgments

This work was supported by the Fundamental Research Funds for the Central Universities (Nos. 2010ZY34, 2011YXL006 and 2011PY0182) and the special fund from the State Key Laboratory of Environmental Aquatic Chemistry, Research Center for Eco-Environmental Sciences, Chinese Academy of Sciences (Nos. 2010-005 and 11K02ESPCR).

References

[1] C.B. Dissanayake, The fluoride problem in the groundwater of Sri Lanka-environmental management and health, Int. J. Environ. Stud. 19 (1991) 195–203.
[2] X. Xu, Q. Li, H. Cui, J. Pang, L. Sun, H. An, J. Zhai, Adsorption of fluoride from aqueous solution on magnesia-loaded fly ash cenospheres, Desalination 272 (2011) 233–239.
[3] D. Banks, C. Reimann, O. Royset, H. Skarphagen, O.M. Saether, Natural concentrations of major and trace elements in some Norwegian bedrock groundwaters, Appl. Geochem. 10 (1995) 1–16.
[4] F. Shen, X. Chen, P. Gao, G. Chen, Electrochemical removal of fluoride ions from industrial wastewater, Chem. Eng. Sci. 58 (2003) 987–993.
[5] R. Liu, J. Guo, H. Tang, Adsorption of fluoride, phosphate, and arsenate ions on a new type of ion exchange fiber, J. Colloid Interface Sci. 248 (2002) 268–274.
[6] P. Battistoni, E. Carniani, V. Fratesi, P. Balboni, P. Tornabuoni, Chemical–physical pretreatment of phosphogypsum leachate, Ind. Eng. Chem. Res. 45 (2006) 3237–3242.
[7] B. Grzmil, J. Wronkowski, Removal of phosphates and fluorides from industrial wastewater, Desalination 189 (2006) 261–268.
[8] J.Y. Park, H.J. Byun, W.H. Choi, W.H. Kang, Cement paste column for simultaneous removal of fluoride, phosphate, and nitrate in acidic wastewater, Chemosphere 70 (2008) 1429–1437.
[9] Warmadewanthi, J.C. Liu, Recovery of phosphate and ammonium as struvite from semiconductor wastewater, Sep. Purif. Technol. 64 (2009) 368–373.
[10] E.J. Reardon, Y. Wang, A limestone reactor for fluoride removal from wastewaters, Environ. Sci. Technol. 34 (2000) 3247–3253.
[11] Y. Cengeloglu, E. Kir, M. Ersoz, Removal of fluoride from aqueous solution by using red mud, Sep. Purif. Technol. 28 (2002) 81–86.
[12] E. Oguz, Adsorption of fluoride on gas concrete materials, J. Hazard. Mater. B 117 (2005) 227–233.
[13] F. Durmaz, H. Kara, Y. Cengeloglu, M. Ersoz, Fluoride removal by Donnan dialysis with anion exchange membranes, Desalination 177 (2005) 51–57.

[14] N. Kabay, O. Arar, S. Samatya, U. Yuksel, M. Yuksel, Separation of fluoride from aqueous solution by electrodialysis: effect of process parameters and other ionic species, J. Hazard. Mater. 153 (2008) 107–113.
[15] P.I. Ndiaye, P. Moulin, L. Dominguez, J.C. Millet, F. Charbit, Removal of fluoride from electronic industrial effluent by RO membrane separation, Desalination 173 (2005) 25–32.
[16] R. Simons, Trace element removal from ash dam waters by nanofiltration and diffusion dialysis, Desalination 89 (1993) 325–341.
[17] N. Mameri, H. Lounici, D. Belhocine, H. Grib, D.L. Piron, Y. Yahiat, Defluoridation of Sahara water by small plant electrocoagulation using bipolar aluminium electrodes, Sep. Purif. Technol. 24 (2001) 113–119.
[18] L. Guo, B.J. Hunt, P.H. Santsci, Ultrafiltration behavior of major ions (Na, Ca, Mg, F, Cl, and SO_4) in natural waters, Water Res. 35 (2001) 1500–1508.
[19] L.E. De-Bashan, Y. Bashan, Recent advances in removing phosphorus from wastewater and its future use as fertilizer (1997–2003), Water Res. 38 (2004) 4222–4246.
[20] N. Bektaş, H. Akbulut, H. Inan, A. Dimoglo, Removal of phosphate from aqueous solutions by electro-coagulation, J. Hazard. Mater. 106 (2004) 101–105.
[21] E. Yildiz, Phosphate removal from water by fly ash using crossflow microfiltration, Sep. Purif. Technol. 35 (2004) 241–252.
[22] H.-G. Kim, H.-N. Jang, H.-M. Kim, D.-S. Lee, T.-H. Chung, Effect of an electro phosphorous removal process on phosphorous removal and membrane permeability in a pilot-scale MBR, Desalination 250 (2010) 629–633.
[23] E.M. van Voorthuizen, A. Zwijnenburg, M. Wessling, Nutrient removal by NF and RO membranes in a decentralized sanitation system, Water Res. 39 (2005) 3657–3667.
[24] J. Lv, K.Y. Wang, T.-S. Chung, Investigation of amphoteric polybenzimidazole (PBI) nanofiltration hollow fiber membrane for both cation and anions removal, J. Membr. Sci. 310 (2008) 557–566.
[25] S.U. Hong, L. Ouyang, M.L. Bruening, Recovery of phosphate using multilayer polyelectrolyte nanofiltration membranes, J. Membr. Sci. 327 (2009) 2–5.
[26] G.S. Zhang, H.J. Liu, R.P. Liu, J.H. Qu, Removal of phosphate from water by a Fe–Mn binary oxide adsorbent, J. Colloid Interface Sci. 335 (2009) 168–174.
[27] A. Eskandarpour, K. Sassa, Y. Bando, H. Ikuta, K. Iwai, M. Okido, S. Asai, Creation of nanomagnetite aggregated iron oxide hydroxide for magnetically removal of fluoride and phosphate from wastewater, Iron Steel Inst. Jpn. 47 (2007) 558–562.
[28] N.C. Lu, J.C. Liu, Removal of phosphate and fluoride from wastewater by a hybrid precipitation–microfiltration process, Sep. Purif. Technol. 74 (2010) 329–335.
[29] D. Dolar, K. Košutić, B. Vučić, RO/NF treatment of wastewater from fertilizer factory-removal of fluoride and phosphate, Desalination 265 (2011) 237–241.
[30] A. Bhatnagar, E. Kumar, M. Sillanpää, Fluoride removal from water by adsorption – A review, Chem. Eng. J. 171 (2011) 811–840.
[31] T. Kwon, G.A. Tsigdinos, T.J. Pinnavaia, Pillaring of layered double hydroxides (LDH's) by polyoxometalate anions, J. Am. Chem. Soc. 110 (1988) 3653–3654.
[32] Z.P. Xu, J. Zhang, M.O. Adebajo, H. Zhang, C. Zhou, Catalytic applications of layered double hydroxides and derivatives, Appl. Clay Sci. 53 (2011) 139–150.
[33] D.G. Evans, X. Duan, Preparation of layered double hydroxides and their applications as additives in polymers, as precursors to magnetic materials and in biology and medicine, Chem. Commun. 5 (2006) 485–496.
[34] V. Rives, Layered Double Hydroxides: Present and Future, Nova Science, New York, 2001.
[35] Y. Wu, Y. Chi, H. Bai, G. Qian, Y. Cao, J. Zhou, Y. Xu, Q. Liu, Z.P. Xu, S. Qiao, Effective removal of selenate from aqueous solutions by the Friedel phase, J. Hazard. Mater. 176 (2010) 193–198.
[36] R. Chitrakar, S. Tezuka, A. Sonoda, K. Sakane, K. Ooi, T. Hirotsu, Synthesis and phosphate uptake behavior of Zr^{4+} incorporated MgAl-layered double hydroxides, J. Colloid Interface Sci. 313 (2007) 53–63.
[37] K.-H. Goh, T.-T. Lim, Influences of co-existing species on the sorption of toxic oxyanions from aqueous solution by nanocrystalline Mg/Al layered double hydroxide, J. Hazard. Mater. 180 (2010) 401–408.
[38] S. Mandal, S. Mayadevi, Adsorption of fluoride ions by Zn–Al layered double hydroxides, Appl. Clay Sci. 40 (2008) 54–62.
[39] S.L. Wang, C.H. Liu, M.K. Wang, Y.H. Chuang, P.N. Chiang, Arsenate adsorption by Mg/Al–NO_3 layered double hydroxides with varying the Mg/Al ratio, Appl. Clay Sci. 43 (2009) 79–85.
[40] L. Lv, J. He, M. Wei, D.G. Evans, Z.L. Zhou, Treatment of high fluoride concentration water by MgAl-CO_3 layered double hydroxides: Kinetic and equilibrium studies, Water Res. 41 (2007) 1534–1542.
[41] K.D. Collins, M.W. Washabaugh, The Hofmeister effect and the behavior of water at interfaces, Quart. Rev. Biophys. 18 (1985) 323–422.
[42] T. Sato, S. Onai, T. Yoshioka, A. Okuwaki, Causticization of sodium carbonate with rock-salt type magnesium aluminium oxide formed by the thermal decomposition of hydrotalcite like layered double hydroxide, J. Chem. Technol. Biotechnol. 57 (1993) 137–140.
[43] N.K. Lazaridis, D.D. Asouhidou, Kinetics of sorptive removal of chromium (VI) from aqueous solutions by calcined Mg–Al–CO_3 hydrotalcite, Water Res. 37 (2003) 2875–2882.
[44] D.P. Das, J. Das, K. Parida, Physicochemical characterization and adsorption behavior of calcined Zn/Al hydrotalcite-like compound (HTlc) towards removal of fluoride from aqueous solution, J. Colloid Interface Sci. 261 (2003) 213–220.
[45] L. Lv, J. He, M. Wei, D.G. Evans, X. Duan, Factors influencing the removal of fluoride from aqueous solution by calcined Mg–Al–CO_3 layered double hydroxides, J. Hazard. Mater. B 133 (2006) 119–128.
[46] S. Miyata, Anion-exchange properties of hydrotalcite-like compounds, Clay Clay Miner. 31 (1983) 305–311.
[47] W.T. Reichle, Anionic clay minerals, Chem. Tech. 16 (1986) 58–63.
[48] APHA, AWWA, WEF, Standard Methods for the Examination of Water and Wastewater, 20th ed., American Public Health Association, Washington, DC, 1998.
[49] J.S. Geelhoed, T. Hiemstra, W.H. Van Riemsdijk, Competitive interaction between phosphate and citrate on goethite, Environ. Sci. Technol. 32 (1998) 2119–2123.
[50] M.A. Ulibarri, M.C. Hermosin, Layered double hydroxides in water decontamination, in: V. Rives (Ed.), Layered Double Hydroxides: Present and Future, Nova Science, New York, 2001, p. 253.
[51] S. Lagergren, Zur theorie der sogenannten adsorption geloester stoffe, Kungliga Svenska Vetenskapsakad Handl. 24 (1898) 1–39.
[52] Y.S. Ho, G. McKay, Pseudo-second order model for sorption processes, Process Biochem. 34 (1999) 451–465.
[53] J. Eastoe, J.S. Dalton, Dynamic surface tension and adsorption mechanisms of surfactants at the air water interface, Adv. J. Colloid Interface Sci. 85 (2000) 103–144.
[54] H. Freundlich, Über die adsorption in lösungen (adsorption in solution), Z. Phys. Chem. 57 (1906) 384–470.
[55] T. Hibino, Y. Yamashita, K. Kosuge, A. Tsunashima, Decarbonation behavior of Mg–Al–CO_3 hydrotalcite-like compounds during heat treatment, Clay Clay Miner. 43 (1995) 427–432.